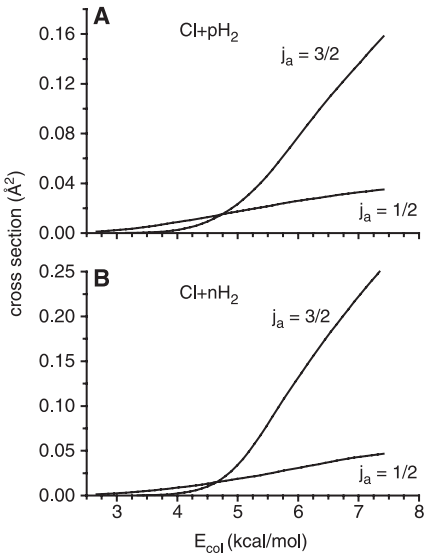

Fig. 5. (**A**) Integral cross sections for reaction of Cl in its ground (j_a = 3/2) and excited (j_a = 1/2) SO state with *p*-H_2. (**B**) Similar integral cross sections for reaction with *n*-H_2. The relative rotational state populations of the j = 0,1 and 2 H_2 rotational levels were taken from (*4*–*6*).

count in Fig. 5, the observed reactivity of the excited SO state will be a factor of 2 less than predicted by Fig. 5.

We predict, fully in agreement with the body of available experimental evidence on other reactions (*25*, *28*), that the adiabatically allowed [$Cl(^2P_{3/2}) + H_2$] reaction will dominate the adiabatically forbidden reaction [$Cl(^2P_{1/2}) + H_2$], except for collision energies below 5 kcal/mol. This prediction is in direct contrast with the recent work of Liu and coworkers (*4*–*6*). This disagreement is one of the major currently unsolved problems in the dynamics of elementary chemical reactions.

Although we predict the reactivity of the adiabatically forbidden channel to be small, we conclude that the breakdown in the BO approximation nevertheless plays an important role in the Cl + H_2 reaction. The coupling between the electronic-orbital angular momentum and the overall orbital motion of the reactants opens up a inelastic channel that competes with reaction. The predicted reactive cross sections are smaller than those calculated from more traditional treatments, in which these nonadiabatic inelastic processes are not taken into account.

We have shown that nonadiabatic processes influence the Cl + H_2 reaction dynamics in subtle and as yet not fully understood ways. In the ab initio calculations of Capecchi and Werner, the nonreactive Π states were characterized only in the reactant arrangement, where these states lie relatively close in energy to the reactive Σ state. It may be that additional electronic couplings at (or inside) the reaction barrier underlie the discrepancy with Liu's experiments. The need for further studies, both theoretical and experimental, is clear.

References and Notes

1. T. C. Allison *et al.*, in *Gas-Phase Reaction Systems: Experiments and Models 100 Years after Max Bodenstein*, H.-R. V. J. Wolfrum, R. Rannacher, J. Warnatz, Eds. (Springer, Heidelberg, Germany, 1996), pp. 111–124.
2. P. Casavecchia, *Rep. Prog. Phys.* **63**, 355 (2000).
3. M. Alagia *et al.*, *Science* **223**, 1519 (1996).
4. S.-H. Lee, L.-H. Lai, K. Liu, H. Chang, *J. Chem. Phys.* **110**, 8229 (1999).
5. S.-H. Lee, K. Liu, *J. Chem. Phys.* **111**, 6253 (1999).
6. F. Dong, S.-H. Lee, K. Liu, *J. Chem. Phys.* **115**, 1197 (2001).
7. F. J. Aoiz, L. Bañares, *J. Phys. Chem.* **100**, 18108 (1996).
8. S. C. Mielke, T. C. Allison, D. G. Truhlar, D. W. Schwenke, *J. Phys. Chem.* **100**, 13588 (1996).
9. H. Wang, W. H. Thompson, W. H. Miller, *J. Chem. Phys.* **107**, 7194 (1997).
10. D. Skouteris *et al.*, *Science* **286**, 1713 (1999).
11. U. Manthe, W. Bian, H.-J. Werner, *Chem. Phys. Lett.* **313**, 647 (1999).
12. N. Balucani *et al.*, *Chem. Phys. Lett.* **328**, 500 (2000).
13. B.-H. Yang, H.-T. Gao, K.-L. Han, J. Z. H. Zhang, *J. Chem. Phys.* **113**, 1434 (2000).
14. D. Skouteris *et al.*, *J. Chem. Phys.* **114**, 10662 (2001).
15. F. J. Aoiz *et al.*, *J. Chem. Phys.* **115**, 2074 (2001).
16. C. Shen, T. Wu, G. Ju, W. Bian, *Chem. Phys.* **272**, 61 (2001).
17. T. C. Allison, G. C. Lynch, D. G. Truhlar, M. S. Gordon, *J. Phys. Chem.* **100**, 13575 (1996).
18. W. Bian, H.-J. Werner, *J. Chem. Phys.* **112**, 220 (2000).
19. F. Rebentrost, W. A. Lester Jr., *J. Chem. Phys.* **63**, 3737 (1975).
20. V. Aquilanti, S. Cavalli, D. De Fazio, A. Volpi, *J. Chem. Phys.* **109**, 3805 (1998).
21. M. H. Alexander, D. E. Manolopoulos, H. J. Werner, *J. Chem. Phys.* **113**, 11084 (2000).
22. M. H. Alexander, B. Pouilly, T. Duhoo, *J. Chem. Phys.* **99**, 1752 (1993).
23. C. E. Moore, *Atomic Energy Levels*, NSRDS-NBS 35 (U. S. Government Printing Office, Washington, DC, 1971).
24. K. E. Shuler, *J. Chem. Phys.* **21**, 624 (1953).
25. R. J. Donovan, D. Husain, *Chem. Rev.* **70**, 489 (1970).
26. D. M. Neumark, A. M. Wodtke, G. N. Robinson, C. C. Hayden, Y. T. Lee, *J. Chem. Phys.* **82**, 3045 (1985).
27. M. Faubel *et al.*, *J. Chem. Phys.* **101**, 2106 (1994).
28. P. J. Dagdigian, M. L. Campbell, *Chem. Rev.* **87**, 1 (1987).
29. G. Capecchi, H.-J. Werner, in preparation.
30. H.-J. Werner, P. J. Knowles, *J. Chem. Phys.* **89**, 5803 (1988).
31. P. J. Knowles, H.-J. Werner, *Chem. Phys. Lett.* **145**, 514 (1988).
32. G. C. Schatz, *J. Phys. Chem.* **99**, 7522 (1995).
33. K. Stark, H.-J. Werner, *J. Chem. Phys.* **104**, 6515 (1996).
34. B. Hartke, H.-J. Werner, *Chem. Phys. Lett.* **280**, 430 (1997).
35. J. F. Castillo, D. E. Manolopoulos, K. Stark, H.-J. Werner, *J. Chem. Phys.* **104**, 6531 (1996).
36. D. Skouteris, J. F. Castillo, D. E. Manolopoulos, *Comput. Phys. Commun.* **133**, 128 (2000).
37. F. J. Aoiz, L. Bañares, J. F. Castillo, *J. Chem. Phys.* **111**, 4013 (1999).
38. B. Pouilly, T. Orlikowski, M. H. Alexander, *J. Phys. B* **18**, 1953 (1985).
39. H. Lefebvre-Brion, R. W. Field, *Perturbations in the Spectra of Diatomic Molecules* (Academic Press, New York, 1986), pp. 118–131.

40. M.H.A. is grateful to NSF for support under grant CHE-9971810. H.J.W. was supported by the Deutsche Forschungsgemeinschaft and the Fonds der Chemischen Industrie. G.C. was supported by a fellowship as a participant in the European Union–Training and Mobility of Researchers network 'Reaction Dynamics,' contract no. HPRN-CT-1999-00007. Finally, the authors are grateful to K. Liu and D. Manolopoulos for their encouragement and for many productive discussions.

1 February 2002; accepted 19 March 2002

Dynamic Aggregation of Chiral Spinners

Bartosz A. Grzybowski* and George M. Whitesides*

An object spinning at the surface of a liquid creates a chiral vortex. If the spinning object is itself chiral, its shape modifies the characteristics of the vortex; interactions between that vortex and other vortices then depend on the chirality of the objects that produce them. This paper describes the aggregation of millimeter-sized, chiral magnetized plates floating at a liquid-air interface and rotating under the influence of a rotating external magnetic field. This external field confines all the plates at densities that cause the vortices they generate to interact strongly. For one set of plates investigated, plates of one chirality attract one another, and plates of the other chirality repel other plates of both chiralities.

The properties and interactions of chiral molecules are a central concern in chemistry, with applications in chromatographic separations, asymmetric catalysis, and medicinal chemistry (*1*, *2*). Chiral interactions between molecules are conceptually well understood (*3*, *4*). Interactions between chiral objects larger than molecules are, however, less well explored or exploited. Here, we describe a study of the interactions between millimeter-scale vortices generated in a fluid by the rotation of chiral objects floating at the surface of that fluid. This system has the characteristics that it is dynamic (*5*–*10*)—that is, the interacting objects (the vortices) exist only when there is a flux of energy into the system—and that both the vortices and the objects that generate them are macroscopic. The system consists of magnetically doped

Department of Chemistry and Chemical Biology, Harvard University, 12 Oxford Street, Cambridge, MA 02138, USA.

*To whom correspondence should be addressed. E-mail: bgrzybowskigmwgroup.harvard.edu (B.A.G.); gwhitesidesgmwgroup.harvard.edu (G.M.W.)

polymeric plates floating at a fluid/air interface and rotating under the influence of an external, rotating magnetic field (Fig. 1). The plates themselves are achiral, but when they are confined to the fluid/air interface, they become chiral. The rotation of the plates generates fluid flows that react differently with the plates of different chiralities.

The millimeter-sized polymeric plates (50 μm thick) were made of epoxy resin doped with magnetite (10% by weight) and were fabricated with a micro transfer molding technique described previously (*11*) (Fig. 1A). The plates were placed at a liquid/air interface [usually a 1:1 by volume mixture of ethylene glycol (EG) and water (*12*)] so that they were fully immersed in the liquid except for their top surface; this geometry minimized capillary interactions between them. Although the plates were slightly more dense than the liquid, they were maintained at the interface by surface tension (*13*). A permanent bar magnet ~5.6 cm long, ~4 cm wide, and ~1 cm thick and with magnetization of ~1000 G/cm^3 (along its longest dimension) was placed below the dish at a distance h (~2 cm) from the interface and rotated with angular velocity ω [at 100 to 600 revolutions per minute (rpm)]. The rotation of the magnet produced an average confining potential (*8*–*10*) that attracted the plates toward the axis of rotation of the magnet. The magnetic moments induced in the plates (*10*, *14*) interacted with the external rotating magnetic field, and the plates spun around their centers of mass with angular frequency equal to that of the external magnet (*15*). The spinning plates interacted with one another hydrodynamically through the vortices they created in the surrounding fluid.

By analogy to chemical notation, we defined the chiralities of the plates with respect to the direction of rotation of the magnetic field as R and S. For the comma-shaped plates, if the tail of a plate points in the direction of rotation of the magnetic field, we designate the plate as R, and if it points in the opposite direction, as S (Fig. 1B).

We visualized the flows around the R and S plates by following the trajectories of small tracer particles at the interface (Fig. 1, B and C). The flow field created by the S isomer was repulsive for all values of ω, and the tracers never came in contact with the plate but instead orbited around it in closed paths. In contrast, an R plate spinning with ω < 450 rpm created a flow that attracted the tracer particles toward it, and they collected in the region between the body and the tail of the plate. For angular speeds ω > 450 rpm, an R plate created a repulsive flow field that was qualitatively similar to that of a spinning circular disk (*8*, *9*).

Multiple plates spinning at the interface interacted with one another hydrodynamically. The nature of these hydrodynamic interactions depended on their chirality and angular velocity ω. At low rotational speeds (ω < 200 rpm; Fig. 2A), the strengths of the vortices produced by the spinners were low, and the hydrodynamic interactions between them were weak. In the absence of strong hydrodynamic repulsions between the plates, the centrosymmetric magnetic force constrained them to a small region near the axis of rotation of the external magnet. The plates occasionally collided with their neighbors and formed disordered aggregates composed of plates of both chiralities; at low values of rotational speeds, the assembly was not selective.

For higher rates of rotation (200 rpm < ω < 450 rpm), the plates aggregated stereo-

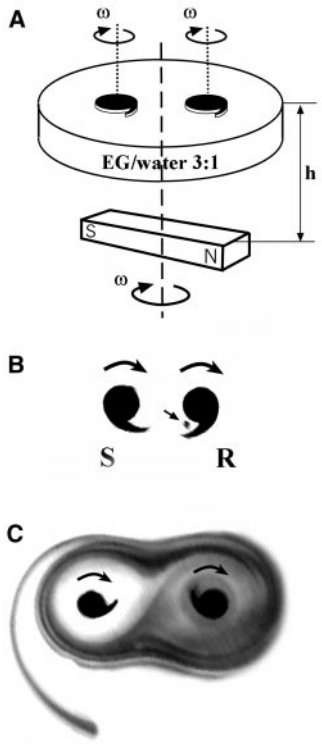

Fig. 1. (**A**) A scheme of the experimental arrangement. A rectangular magnet rotates at ω 100 to 600 rpm below a dish filled with liquid (usually a mixture of EG and water). The distance between the upper face of the magnet and the liquid/air interface is h ~ 20 mm. Magnetically doped polymeric plates (~1 mm in diameter, 50 μm thick) are placed at the interface and are immersed in the liquid except for their top surfaces. The plates spin at angular velocity ω around their axes. The magnetic force F^m attracts the objects towards the center of the dish; the hydrodynamic force F^h between the spinning objects can be either attractive or repulsive, depending on the geometry of the plates and their rotational speed. The drawing in (**B**) defines the chirality of the plates with respect to the direction of rotation of the magnetic field (indicated by arrows around the objects). Tracer particles (10-μm latex spheres) floating at the interface are attracted toward the R isomer but not toward the S isomer. The arrow indicates an aggregate of spheres attracted by R. (**C**) Flowlines around a pair of plates of different chiralities (S on the left, and R on the right) visualized by addition of droplets of crystal violet dye dissolved in the EG/water mixture to the liquid/air interface. The dye moves into contact with the R plate but is not allowed to approach the S plate.

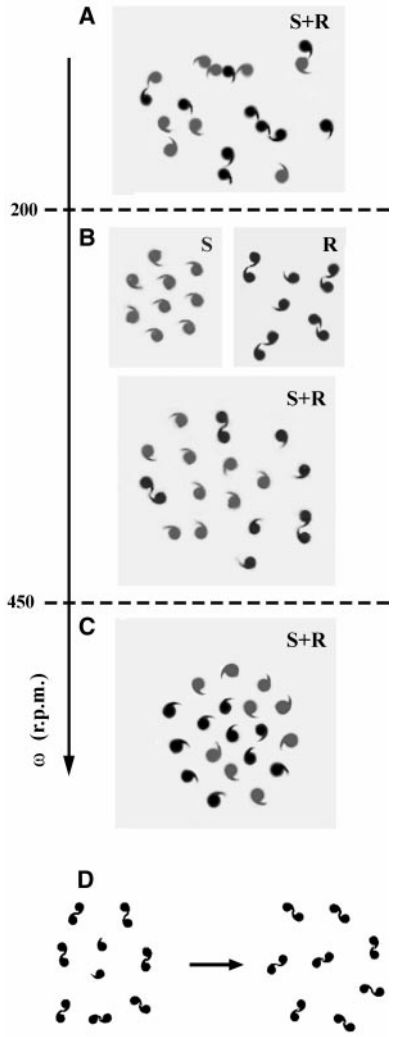

Fig. 2. (**A**) Disordered aggregates formed by 10 R and 9 S commas rotating at ω ~ 200 rpm at the EG-water/air interface. (**B**) Stereoselective aggregation of the plates was observed in the intermediate range of rotational speeds (200 to 450 rpm). For nine S plates spinning at ~300 rpm, the hydrodynamic interactions between the plates are repulsive. In contrast, the 10 R plates attract each other and form dimers. In aggregates composed of both S and R plates, only the R plates that are close to each other form dimers; the S plates repel both R and S. (**C**) At ω > 450 rpm, the plates repel one another (regardless of their chirality) and order into open lattice structures. (**D**) Stable symmetric aggregate of 16 R plates rotating at ω ~ 300 rpm contains unpaired plates. The fully dimerized structure forms when the liquid/air interface is agitated by gently tapping the dish at 5 to 10 Hz.

selectively (Fig. 2B). In this regime, the repulsive hydrodynamic interactions between the plates were strong enough to prevent their random collisions, and the stereoselectivity of aggregation reflected the differences in the flow fields created by the R and S enantiomers. The S commas repelled one another and did not aggregate. In contrast, the R commas attracted other R commas and formed dimers. In aggregates composed of both R and S commas, the R commas that were close to each other dimerized, whereas S and distant R commas remained separated monomers. For $\omega > 450$ rpm, the hydrodynamic interactions between the plates of both chiralities were repulsive. The open lattice structures that organized (Fig. 2C) were similar to those formed by the same numbers of spinning disks (*8*).

We studied the mechanism of dimerization of the R commas in the intermediate range of rotation rates. Three R plates is the smallest assembly in which spontaneous dimerization occurs; two R plates do not dimerize. For a pair of R isomers, the plates oscillate in phase and occasionally come into close proximity, but they never come into permanent contact. For three plates, the motion is complex: One plate catalyzes the dimerization of the other two. Initially, as the plates spin, they self-organize so that two of them are in phase (their tails point in the same direction) with respect to each other, and they are both in antiphase (tails pointing in opposite directions) with respect to the third plate. The antiphase orientation is a prerequisite for dimerization. Once in the proper orientation, one of the pair of antiphase plates begins to oscillate along the line joining their centers. The amplitude of this oscillation varies with time and depends on the orientation of the third plate with respect to the oscillating pair. When the pair is oriented with the tails pointing toward each other, and if the tail of the third plate is perpendicular to the axis of oscillation, the ends of the tails of the oscillating plates come into contact and a dimer forms. The dimer readjusts its shape slightly so that the angle between the tails of its constituent monomers is oblique; this arrangement is stable and appears to minimize the hydrodynamic resistance of the spinning adduct. The unused R plate orbits around the dimer. From these observations, we conclude that (i) dimerization of R plates is a cooperative phenomenon; each dimerizing pair requires a "chaperon" plate(s) that "catalyzes" the transformation by disturbing the flow field in the vicinity of the reacting pair; and (ii) the plates must be in specific mutual orientations in order to dimerize.

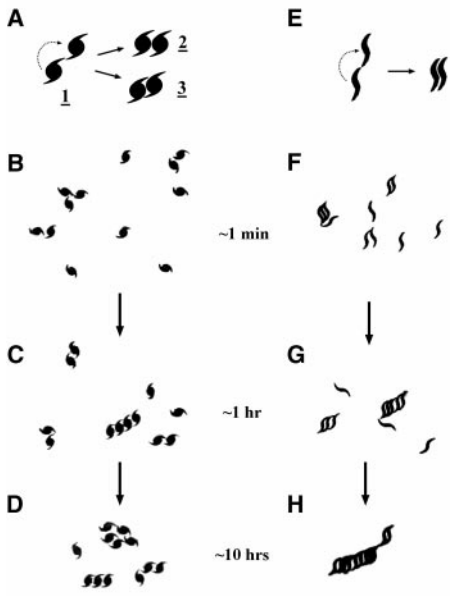

Fig. 3. Assembly of R structures having two oppositely directed tails and spinning at the EG-water/air interface at $\omega \sim 300$ rpm. (**A**) Schematic illustration of the conformational rearrangement of a tail-to-tail dimer (left) into two possible side-to-side forms. After initial dimerization and occasionally trimerization (**B**), the plates form extended structures such as those shown in (**C**) and (**D**). These structures can be single-stranded (straight or slightly curved) or double-stranded (**E** to **H**). Formation of extended linear structures by thin propeller plates. In the end, one aggregate with the majority of plates stacked side-to-side is formed. The formation of higher aggregates is a reversible process, and large aggregates can spontaneously fragment into smaller structures; the mismatched connections [such as in the left structure in (F)] are easiest to break. The aggregation is a self-correcting process that favors extended linear structures with plates oriented side-to-side.

Dimerization of the R commas modifies the forces acting in the system: Unlike the monomers that attract each other, the dimers repel their neighbors. In ensembles composed of R plates only (Fig. 2D), the first two dimers form within seconds of the start of rotation. These initial dimers repel the remaining monomers hydrodynamically. The probability of two monomers being close to each other (and reacting) thus decreases, and the pairing process slows down. After several hours, an aggregate of stable morphology is formed. Regardless of the number of plates used, the final system contains unpaired plates: Spontaneous dimerization never goes to completion. In the final aggregate, the spinning objects (monomers and dimers) organize into a symmetric superstructure (Fig. 2D, left). The nearly symmetric flow fields around the monomers prevent further pairing. Dimerization can be pushed to completion if the symmetry of this superstructure is broken by an external disturbance; for example, by gentle agitation of the liquid surface (Fig. 2D, right).

After forming a tail-to-tail connection, the comma-shaped plates have no other points of attachment for connection to other plates. We expected that R isomers of propeller-shaped plates—that is, plates analogous to those having a comma shape but with two tails—would form structures with more than two components (Fig. 3). After the initial formation of dimers and occasionally trimers, plates of this shape are still capable of forming connections to other plates. The mode of connection, however, is different than in comma-shaped plates. The structure that forms initially but transitorially is 1 (Fig. 3A). Its longest dimension is significantly larger than that of a dimer of comma-shaped plates, and it must overcome higher hydrodynamic resistance during rotary motion against the fluid. The hydrodynamic drag is minimized by a change in conformation to 2 (major product) or 3 (minor product); these conformations are more compact, have a much smaller hydrodynamic radius, and are stable. The stable dimeric forms still have two tails available with which they can connect with other plates, and the resulting higher aggregates [trimers and tetramers (Fig. 3, B and C)] appear as linear structures. With time, however, some of these linear assemblies convert to more compact, two-line aggregates (Fig. 3D).

The R propeller-shaped plates can form several final structures. Thinner propellers form extended linear assemblies (Fig. 3E). These propellers dimerize exclusively in a side-to-side conformation and yield straight aggregates (Fig. 3, F through H). Unlike the comma plates, thin propellers do not require "catalysis" by neighboring spinners to dimerize: For $\omega < 450$ rpm, dimerization is spontaneous. The initial symmetric configuration of synchronized monomers rotating in phase can sometimes be achieved and sustained for several seconds, but inevitably one (or more) of the plates falls out of phase with its neighbors and dimerizes.

In contrast to a dimer of comma plates that creates a repulsive flow field around it, the dimer of propellers attracts remaining monomers. Because large aggregates of propeller plates occasionally fall out of resonance with the external magnetic field and rotate more slowly than it does (or even temporarily stop rotating), the repulsive forces they exert on other pieces decrease; the decrease in hydrodynamic repulsion facilitates the addition of monomers to already existing assemblies. Also, because the area swept by a rotating dimer (or higher aggregate) is larger than that swept by a monomer, the probability that it will encounter a monomer and engage it increases with the increasing size of an aggregate. Both of these effects contribute to the positive feedback in this system: The probability of addition increases with the increasing size of an already formed structure.

Aggregation of the propeller plates (both the thick and the thin ones) is not as stereoselective

as that of the comma plates. When no R plates are present, the S propellers repel one another, and above $\omega \sim 200$ rpm they form open lattice structures, whereas at lower rotational rates, the hydrodynamic repulsions are weak and the plates form disordered structures. In the mixed ensembles of R and S isomers, however, the S propellers occasionally participate in aggregation and attach to large aggregates of R plates, especially when the rotation of the aggregate is not resonant with the external field. The selectivity improves with decreasing viscosity of the liquid. In pure water, even the large assemblies rotate fast, and we observed that in ~50% of experiments all the S propellers remained monomers.

We have described a rationally designed dynamic system in which the aggregation of macroscopic particles is mediated by chiral vortex-vortex interactions. We found that both chirality and the energetics of the components of this system are the key variables that control the formation of extended structures. We believe that this system and others analogous to it can be used to model certain aspects of stereoselective self-assembly in molecular ensembles. Indeed, recent results of Ribo *et al.* (*16*) suggested that stereoselective aggregation of certain chiral molecules in rotating liquids could have its origin in the vortex-vortex interactions between them. We also believe that our observations will stimulate research in fluid mechanics that will ultimately allow theoretical description of the forces acting between vortex patches (*17*, *18*) generated by rotating objects of complex shapes.

References and Notes

1. M. R. Islam, J. G. Mahdi, I.D. Bowden, *Drug Safety* **17**, 149 (1997).
2. R. Noyori, T. Ohkuma, *Angew. Chem. Int. Ed. Engl.* **40**, 40 (2001).
3. K. B. Lipkowitz, *Acc. Chem. Res.* **33**, 555 (2000).
4. J. A. Gladysz, B. J. Boone, *Angew. Chem. Int. Ed. Engl.* **36**, 551 (1997).
5. M. Straskraba, S. E. Jorgensen, B. C. Patten, *Ecol. Model.* **117**, 3 (1999).
6. P. Winiwarter, C. Cempel, *Syst. Res.* **9**, 9 (1992).
7. M. C. Cross, P. C. Hohenberg, *Rev. Mod. Phys.* **65**, 851 (1993).
8. B. A. Grzybowski, H. A. Stone, G. M. Whitesides, *Nature* **405**, 1033 (2000).
9. B. A. Grzybowski, J. Jiang, H. A. Stone, G. M. Whitesides, *Phys. Rev. E* **46**, 11603 (2001).
10. B. A. Grzybowski, G. M. Whitesides, *J. Phys. Chem. B* **106**, 1188 (2002).
11. The plates were prepared with a micro transfer molding technique described in detail in Y. Xia, G. M. Whitesides, *Angew. Chem. Int. Ed. Engl.* **37**, 550 (1998).
12. The kinematic viscosity of the mixture affected the stability of the aggregates. In liquids of low viscosities [$\upsilon < \sim 3$ centipoise (cP)], the flows created by spinning disks were often turbulent, and the self-assembled aggregates were unstable. If the viscosity was too high ($\upsilon > \sim 50$ cP), the magnetic torque was to small to spin the disks. Most stable structures were observed in liquids of intermediate kinematic viscosities, such as the 1:1 mixture of EG and water.
13. B. A. Grzybowski, N. Bowden, F. Arias, H. Yang, G. M. Whitesides, *J. Phys. Chem. B* **105**, 404 (2001).
14. The magnetite particles were uniformly distributed in the polymer matrix, and no long-range order existed between magnetic domains. The typical size of a magnetite grain was ~100 Å. The grains were fixed in the polymer; that is, they did not rotate in response to the changes in the external magnetic field.
15. For the typical rotational speeds ($\omega \sim 100$ to 600 rpm), particle radii ($a \sim 1$ mm), and fluid kinematic viscosities of our experiments ($\upsilon \sim 0.1$ cm^2/s), the Reynolds numbers on the scale of the rotating particles ($\mathrm{Re} = \omega a^2/\upsilon$) were between 1 and 5.
16. J. M. Ribo, J. Crustas, F. Sagues, J. Claret, R. Rubires, *Science* **292**, 2063 (2001).
17. T. H. Havelock, *Philos. Mag.* **11**, 617 (1931).
18. D. G. Dritschel, *J. Fluid Mech.* **157**, 95 (1985).

19. Supported by the U.S. Department of Energy (contract no. 00ER45852).

16 November 2001; accepted 19 March 2002

Thermochemistry and Aqueous Solubilities of Hydrotalcite-Like Solids

Rama kumar Allada,[1] Alexandra Navrotsky,[1]* Hillary Thompson Berbeco,[2] William H. Casey[3,4]

Hydrotalcites are used in technology as catalysts and anion exchangers and are important sinks for environmental contaminants. Their compositional variability makes it important, but difficult, to estimate their aqueous solubility. We report calorimetric measurements of the heats of formation of cobalt-aluminum hydrotalcite phases. The heat and free energy of formation from the elements are equal to those of mechanical mixtures of binary compounds, namely hydroxides and carbonates. The interlayer anion is much more important than the cation in determining the solubility of the hydrotalcite phase and its ability to contain or release heavy metals to the environment. Because hydrotalcites do not have an unreactive polymer as a structural core, their aqueous stability will change dramatically with composition, particularly with anion content. This simple mechanical mixture model allows prediction of aqueous solubilities and trace metal retention in a variety of geochemical settings.

In 1995, d'Espinose de la Caillerie (*1*, *2*) showed that the uptake of divalent metals by aluminum (hydr)oxide minerals was commonly due to precipitation of hydrotalcite-like minerals and not to the formation of an adsorbate surface complex as previously thought. These results are now confirmed and extended (*3*–*8*) and are important to geochemistry because predictions of total metal concentrations in aquifers usually rely on the calculated solubilities of minerals with fixed composition in the natural water. The mineral phases considered are usually simple hydroxides, carbonates, sulfates, and so forth, for which thermodynamic data are available. Solids of variable composition, like those of the hydrotalcite class, are usually ignored because accurate thermodynamic data are missing or difficult to acquire (*9*). Because the rates of metal migration in soil and their bioavailability are usually proportional to the equilibrium concentration, it is important to identify trace mineral phases that might exert a disproportionate effect on the equilibrium metal concentration. Particularly important are minerals that reduce the total concentration of the dissolved metal in solution relative to equilibrium with simple phases, because these reactions directly influence our assessments of environmental safety.

Hydrotalcites have the general stoichiometry: $M(II)_{1-x}M(III)_x(OH)_2[A^{n-}]_{x/n}\cdot mH_2O$ and a structure composed of positively charged brucite-type metal-hydroxide layers intercalated with anions [A^{n-}] and water molecules. The structures accommodate a number of cations, including Mn^{2+}, Mg^{2+}, Co^{2+}, Ni^{2+}, Zn^{2+}, Fe^{2+}, Al^{3+}, Fe^{3+}, Cr^{3+}; interlayer anions such as CO_3^{2-}, NO_3^-, Cl^-, and SO_4^{2-}; and varying amounts of water (*5*, *10*). Thermodynamic data are not available because hydrotalcites exhibit wide compositional variations, are disordered, and readily exchange anions. A means of estimating thermodynamic data for many such compounds based on measurements for only a few would be very useful.

As a first step in obtaining thermochemical data and devising a systematic thermodynamic model, we measured enthalpies of for-

[1]Thermochemistry Facility, Department of Chemical Engineering and Materials Science, University of California, Davis, CA 95616, USA. [2]Franklin W. Olin College of Engineering, Needham, MA 02492, USA. [3]Department of Land Air and Water Resources, [4]Department of Geology, University of California, Davis, CA 95616, USA.

*To whom correspondence should be addressed. E-mail: anavrotsky@ucdavis.edu